CSMA 2015
12 Colloque National en Calcul des Structures
18-22 Mai 2015, Presqu'île de Giens (Var)

Experimental Tuned Mass Damper Based on Eddy Currents Damping Effect and Adjustable Stiffness

S. Lo Feudo [1,2], A. Allani [1], G. Cumunel [1]
P. Argoul [1], D. Bruno [2]

[1] *Université Paris-Est, Laboratoire Navier (UMR 8205), CNRS, ENPC, IFSTTAR*
{anissa.allani,pierre.argoul,gwendal.cumunel}@enpc.fr
[2] *DINCI, Università della Calabria, {stefania.lofeudo,d.bruno}@unical.it*

Abstract — An experimental Tuned Mass Damper (TMD) is proposed in order to damp vibrations induced by external excitations. This TMD is based on the Eddy Currents damping effect and is designed in such a way as to allow a manually adjustment of its own stiffness and inherent damping. The TMD's modal parameters estimation is therefore carried out by applying the Continuous Wavelet Transform to the signals obtained experimentally. The influence of the manual adjustment of the TMD's components on its dynamical properties is then studied.
Key words — TMD, Eddy currents, vibration control, wavelet transform

1. Introduction

In the framework of vibration control of civil engineering structures, an important role is covered by the adoption of devices called Tuned Mass Damper (TMD). The basic idea consists in attach a passive control device to a primary structure, for example a tall building or a bridge, which is tuned with the main structure's natural frequency and is able to reduce vibrations induced by harmonic excitation, wind loads and/or earthquake ground motions. Part of the vibration energy can be in fact transferred from the principal structure to the TMD, so that the capability to dissipate energy is improved, with obvious advantages in terms of durability and structural safety.

In this research, an innovative experimental TMD is proposed and designed to be placed on a top floor of building scale model. The proposed TMD is manufactured in such a way as to allow a change in the dynamical properties of the device itself, namely the stiffness and the damping coefficient. In fact, since the mass of the TMD is fixed for practical issues, TMD's stiffness and damping represent the design parameters, so that it is necessary to easily set them in order to test some of the optimization criteria proposed in the literature and reviewed by Allani et al. [1].

The damping of the TMD is obtained with eddy currents damping effect. In particular, when a conductive material is subjected to a time-varying magnetic field, due to the electromagnetic induction an electromotive force (emf) is produced in the conductor, and eddy currents are generated. According to the Faraday's law of induction, this electromotive force opposes the rate of change with respect to time of the magnetic flux. Moreover, for the Lenz's law, the consequent currents circulate in such a way as to generate a magnetic field that opposes the original change in magnetic flux. For this reason, when the flux rises the emf is negative and the eddy currents contrast this flux increase. The currents circulation causes therefore a magnetic field which flux is opposed to the other. Conversely, when the flux rate drops, the emf is positive and eddy currents generate a magnetic field which flux is concordant with the other. In addition, a Lorentz force appears contrasting the motion but owing to the resistance of the conductor, energy is dissipated into heat, so that a vibration reduction is achieved. According to Graves et al., [6], electromagnetic dampers can be based on motional or transformer electromotive force depending on the mechanism that generates the emf. The transformer emf devices generate an emf in presence of a stationary conducting circuit and of a time-varying magnetic field

linking the circuit, whereas the motional emf devices generate an emf within a conductor moving through a stationary magnetic field. The authors remarked that, although the transformer emf devices are more efficient, the motional emf are more suitable to realistic situations. Some researches related to the use of the eddy currents damping mechanism were then reviewed by Sodano & Bae in [9]. As advantages of adopting this damping strategy, the authors highlighted the lack of contact between the eddy current damper and the system to damp, so that not only the dynamical response and the material properties are unaffected by its addition, but also the damper performance does not degrade over the time. As far as the vibration control is concerned, Larose et al. adopted in [7] a TMD to reduce the oscillations of a full-bridge aeroelastic model, providing the adjustable inherent damping of the added mass by an eddy currents mechanism. An eddy currents damper was also proposed by Sodano et al. in [10] with the aim to suppress vibration of a beam in case of permanent magnet placed on the top of the beam and sets perpendicular to the beam's vibration direction. In this case, only the radial component of the magnet flux generates the damping force since the magnetic flux density component parallel to the velocity of the conducting sheet does not produce any contribution. In order to measure the damping of the beam as a function of the gap between the used copper plate and the surface of the magnet, Sodano et al. had calculated the damping ratio either by determining the logarithmic decrements of the initial condition response and by applying the unified matrix polynomial approach to the frequency response. According to them, eddy currents increase greatly the damping and the eddy current damping force is highly non-linear with respect to the gap between the magnet and the beam. Ebrahimi et al. had studied in [5] the problem of a magnetic shock absorber based on the motional emf, and Bae et al. also proposed in [2] a theoretical model able to predict the eddy current damping effect on the suppression of a cantilever beam vibrations. A magnetically TMD was also recently tested in case of a large beam by Bae et al. [4]. Finally, a large-scale horizontal TMD based on eddy current damping was designed and tested by Wang et al. in [11]. The damping ratio of the TMD was evaluated by using the logarithmic decrements obtained from free vibrations test data, and it was showed to radically drop as the gap between magnet and conductive mass increases. A feasibility analysis was also carried out by considering durability and economic viability of such a TMD.

The present work is arranged as follows: Section 2 provides a general theoretical background on eddy currents and on the methods adopted for the TMD's parameter estimation; Section 3 illustrates the proposed experimental TMD model together with the achieved results and finally, Section 4 gives some concluding remarks.

2. Eddy currents Tuned Mass Damper

When a conductive material moves along a stationary magnetic field, eddy currents are induced, (Figure 1.a). By neglecting the surface charge in the conductive plate, the eddy currents density can be written as:

$$\mathbf{J} = \sigma(\mathbf{v} \times \mathbf{B}) \tag{1}$$

where σ is the electrical conductivity of the conductive material, $\mathbf{v} = (v_x + v_y + v_z)^T$ is the relative velocity between the permanent magnet and the conductor, $\mathbf{B} = (B_x + B_y + B_z)^T$ is the magnetic flux density due to the magnet and $\mathbf{v} \times \mathbf{B}$ represents the electromotive force driving the eddy currents. Considering that velocity has component only in the x direction, the currents density is given by:

$$\mathbf{J} = \sigma v_x (-B_z \mathbf{j} + B_y \mathbf{k}) \tag{2}$$

The magnetic flux density components due to a permanent circular magnet can be evaluated by applying the Biot-Savart law to a circular loop as follows:

$$d\mathbf{B} = \frac{\mu_0 M dz}{4\pi} \oint \frac{d\boldsymbol{s} \times \mathbf{R}_1}{\mathbf{R}_1^3} \tag{3}$$

where μ_0 is the permeability, M the magnetization per unit length and dz a differential length in the magnet thickness direction.

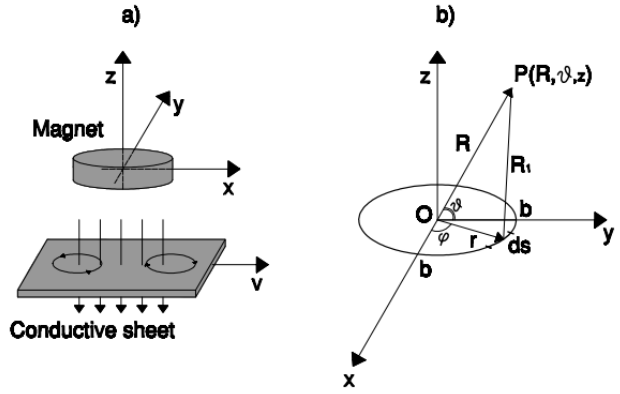

Figure 1 – a) Eddy currents mechanism and b) circular magnetized strip

In order to evaluate $d\mathbf{B}$ at a point $P(R,\theta,z)$, it is useful to adopt a cylindrical coordinate system defined by (Figure 1.b):

$$\begin{aligned} &\mathbf{R}_1 = \mathbf{R} - \mathbf{r}, \quad \mathbf{r} = b\cos\phi\mathbf{i} + b\sin\phi\mathbf{j} \\ &\mathbf{R} = y\mathbf{j} + z\mathbf{k}, \quad d\boldsymbol{s} = -b\sin\phi d\phi\mathbf{i} + b\cos\phi d\phi\mathbf{j} \end{aligned} \tag{4}$$

where $\mathbf{R}_1$ is the distance between an infinitesimal element $d\boldsymbol{s}$ on the strip and the point P on the (yz)-plane, $\mathbf{R}$ the distance of P from the center of the circular magnet and b its radius. By substituting Eqs. (4) into Eq. (3) and integrating through the magnet thickness, the magnetic flux density due to the permanent circular magnet can be expressed as [3, 10]

$$B_x = \int dB_x = \frac{\mu_0 M}{4\pi} \int_{-h/2}^{h/2} \int_0^{2\pi} bz \left[\frac{\cos\phi}{(y^2 + z^2 + b^2 - 2by\sin\phi)^{3/2}} \right] d\phi dz$$

$$B_y = \int dB_y = \frac{\mu_0 M}{4\pi} \int_{-h/2}^{h/2} \int_0^{2\pi} bz \left[\frac{\sin\phi}{(y^2 + z^2 + b^2 - 2by\sin\phi)^{3/2}} \right] d\phi dz$$

$$B_z = \int dB_z = \frac{\mu_0 M}{4\pi} \int_{-h/2}^{h/2} \int_0^{2\pi} b \left[\frac{b - y\sin\phi}{(y^2 + z^2 + b^2 - 2by\sin\phi)^{3/2}} \right] d\phi dz$$

The eddy currents $\mathbf{J}$ produce in turn a magnetic field with opposite polarity with respect to those generated by the permanent magnet, and a repulsive force appears. This force can be evaluated by adopting the Lorentz's Law and can be expressed as follows:

$$\mathbf{F} = \int_V (\mathbf{J} \times \mathbf{B})\, dV \tag{5}$$

where V is the conductor volume. Substituting Eq. (2) into Eq. (5) and by doing the cross product, the electromagnetic force becomes

$$\mathbf{F} = \sigma v_x \int_V [(-B_z^2 - B_y^2)\mathbf{i} + B_x B_y \mathbf{j} + B_x B_z \mathbf{k}]\, dV$$

Hence, according to [11] and by virtue of Eq. (2), the x component of the electromagnetic force does not depend on the component of the magnetic field parallel to the velocity of the conductor, B_x:

$$F_x = -\sigma v_x \int_V (B_y^2 + B_z^2)\, dV$$

The damping force in the x direction is thus proportional to the velocity vector with opposite direction. It is therefore possible to define the linear damping coefficient and the damping ratio of the TMD [11] as follows:

$$C_{TMD} = \sigma \int_V (B_y^2 + B_z^2)\, dV, \quad \xi_{TMD} = \frac{C_{TMD}}{2\omega_{TMD} m_{TMD}}$$

where m_{TMD} and ω_{TMD} are the mass and the natural frequency of the TMD, respectively.

2.1. Parameter estimation

The numerical evaluation of the frequency and of the damping ratio is carried out by applying both a classical method and the Continuous Wavelet Transform (CWT) on experimental data. The first method consists in evaluating the natural period of the system from a free vibration test by measuring the distance between two peaks in the temporal domain, and the damping ratio by applying the logarithmic decrement technique. In addition, the modal parameters identification from experimental data is also performed by applying the CWT to the achieved signals. The CWT allows to study a signal in a time-frequency plane, allowing the time evolution estimation of natural frequencies, damping ratios and mode shapes, which is useful for noised and non-stationary or non-linear systems. Generally speaking, the CWT of a signal consists in the decomposition of the signal itself in a family of function localized in time and in frequency, called wavelet. A wavelet family is built by scaling and shifting in time a base wavelet, called mother wavelet. The principal characteristic of the mother wavelet is to have zero mean and finite energy. In this way, the signal can be analyzed at different scales, with large windows for low frequencies and narrow windows for high frequencies. In particular, the CWT of an asymptotic signal is concentrated along some curves in the time-frequency domain called ridges, and the restriction of the CWT to each ridge is called skeleton of the wavelet. The skeleton gives the natural frequency of the signal, whereas the time evolution of the logarithm of the Wavelet transform amplitude gives information about damping, for further explanation please see Le & Argoul [8].

3. Experimental TMD model

The proposed TMD is made of a $150\ g$ copper mass supported by two thin aluminum sheets. The device was designed in order to permit a manual adjustment of the natural frequency and of the inherent damping, and to be placed on the top floor of a building scale model (Figure 2). One of the cable's support position is variable, so that the amount of stretch in the slender cable can be manually changed. As long as the cable tensile stress is increased, the TMD stiffness rises, as well as the natural frequency. In this study, by considering the frequency bandwidth of interest, the support is supposed to move over a range of $0.4\ mm$ and the step size here considered is of $0.04\ mm$. This range will be denoted hereafter as D_1. In particular, when D_1 is sets equal to $0\ mm$, the TMD frequency is the higher among those considered. The damping of the TMD is conversely given by a magnet located up to the mass, which distance is adjustable. Since the conductive material, that is the copper mass, is subjected to a time-varying magnetic field, eddy currents are induced in the conductor. The time-

varying magnetic field is in fact generated by the oscillation of the conductor in the stationary field and the normal of the magnet surface is perpendicular to the velocity. The magnet is therefore moved over a range of $2\,mm$, and the step size adopted here is of $0.2\,mm$. This range will be denoted hereafter as D_2. The initial chosen value of D_2 corresponds to a distance between the magnet and the mass of $3.35\,mm$.

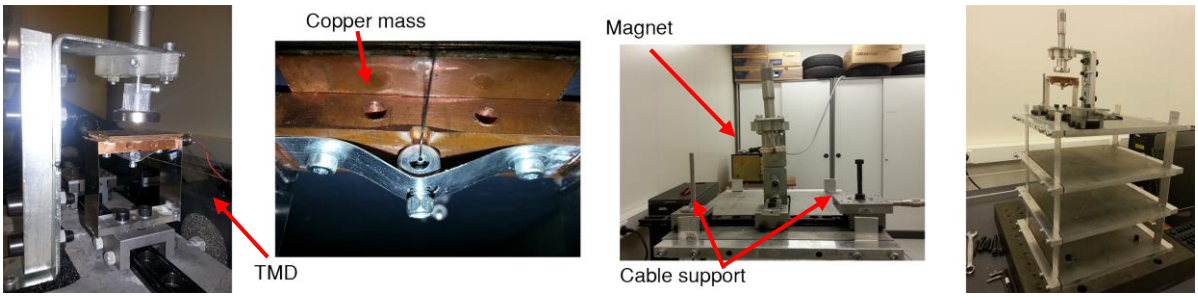

Figure 2 – Eddy Currents Tuned Mass Damper

3.1. Parameters estimation

In order to set the TMD with optimal parameters, it is necessary to characterize the TMD properties behavior when the magnet distance and the stretch in the cable are changed. To this end, the response of the TMD alone was recorded in several free vibration test when an impulsive shock is applied on it. For each fixed value of D_1 the response of the TMD in the temporal domain was measured by varying D_2 and each test was carried out three times. The signals recorded were then cut at the two ends to eliminate superfluous recordings, and a high-pass filter was adopted in order to remove a low frequency component deriving probably from external factors. The obtained smoothed and filtered data were therefore adopted in order to evaluate the TMD's damping ratio and frequency by using the CWT. The CWT of a signal allows not only to evaluate the modal parameters of the system, but also to appreciate their evolution in time. This represents an important issue in this context since TMD performance is very sensitive to a change in the parameters characteristics. The Cauchy wavelet was chosen as mother wavelet and the Q factor, which represents the ratio of the center-frequency to the frequency bandwidth, was set equal to 10 (for more details please see [8]).

In Figures 3 and 4, results are presented for two cases where the obtained damped frequency is in the neighborhood of the fundamental frequency of the structure to be controlled, which is $10.77\ Hz$. By looking at the ridge of the CWT, it emerges that the frequency keeps almost constant with time and the damping ratio, which can evaluated from the slope of the logarithm of the Wavelet transform modulus exhibits in the first instants a non-linear behavior due probably to geometric non-linearity. However, the non-linear effect keeps out of the zone of interest since the considered domain was chosen in such a way to neglect the so-called edge effect. By looking at the logarithmic of the amplitude of the Wavelet transform, it appears that the damping can be correctly modeled as viscous since the logarithmic of the amplitude has a linear behavior within the considered domain. In Figure 5, the TMD acceleration, the damping ratio and the natural frequency of damped vibration are shown within the considered domain and neglecting the edge effect. In Figure 5.a, the signal's peaks are detected, and in Figure 5.b, the damping ratio obtained from the CWT and from the logarithmic decrement are compared. Finally in Figure 5.c, the damped frequency achieved by applying the CWT and that obtained from the peak distance are presented. From Figure 5.b it emerges that the damping ratio obtained from the logarithmic decrement technique has an oscillatory behavior around the value obtained from the Wavelet transform. Also the damped frequency achieved from the peaks distance has an oscillatory behavior, but values are very close. In Figure 6, for a fixed D_1, the damped frequency and the damping ratio, by varying the magnet distance, are shown when both methods are

used. Results obtained from the classical methods slightly underestimate those obtained by the Wavelet transform, but the global trend appears to be quite similar. In Figure 7, results obtained in terms of modal parameters for each D_1 and D_2 value considered are summarized. The damped frequency and the damping ratio reported are the average values obtained from each of the three tests, as in Figure 6. In Figure 7.a it appears how, for a fixed tension in the cable D_1, the frequency remains nearly constant by varying the distance of the magnet. The damped frequency also varies linearly by changing D_1 and it does not depend on the magnet distance. Conversely, Figure 7.b shows how the damping ratio varies in a non-linear way with respect to D_1 and D_2. In particular, when the magnet is close to the conductor, the damping ratio tends to assume higher values.

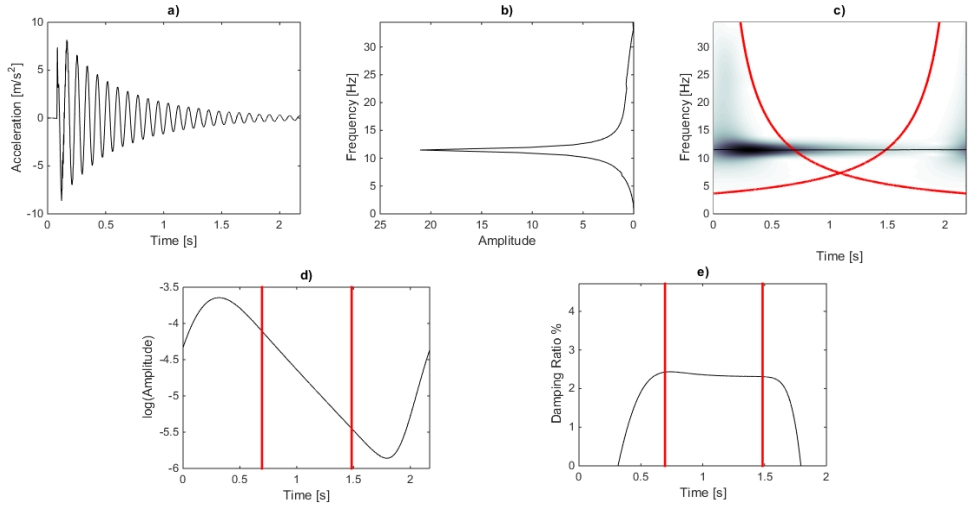

Figure 3 – a) TMD's acceleration, b) Fourier transform, c) CWT, d) Logarithmic plot of the skeleton amplitudes and e) damping ratio of the TMD under an impulsive shock for $D_1 = 0.04\ mm$ and $D_2 = 3.55\ mm$

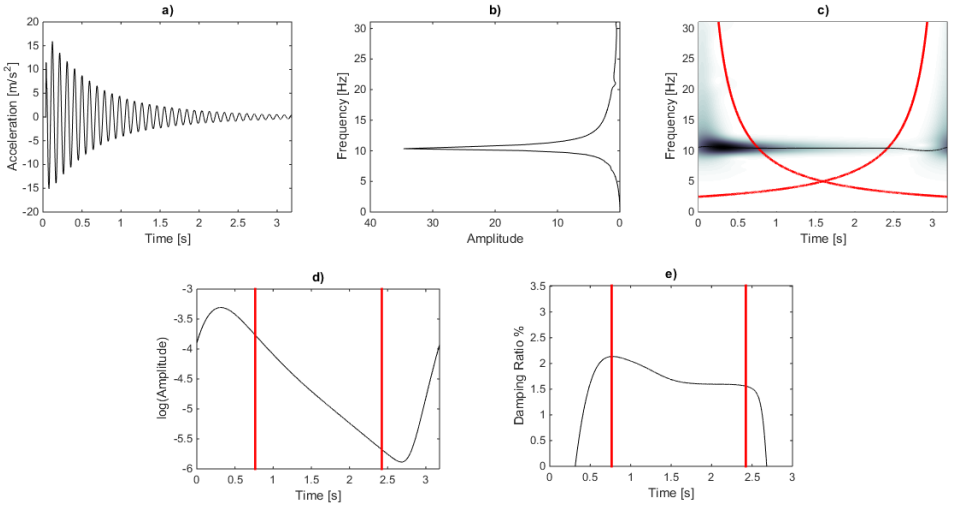

Figure 4 – a) TMD's acceleration, b) Fourier transform, c) CWT, d) Logarithmic plot of the skeleton amplitudes and e) damping ratio of the TMD under an impulsive shock for $D_1 = 0.24\ mm$ and $D_2 = 5.15\ mm$

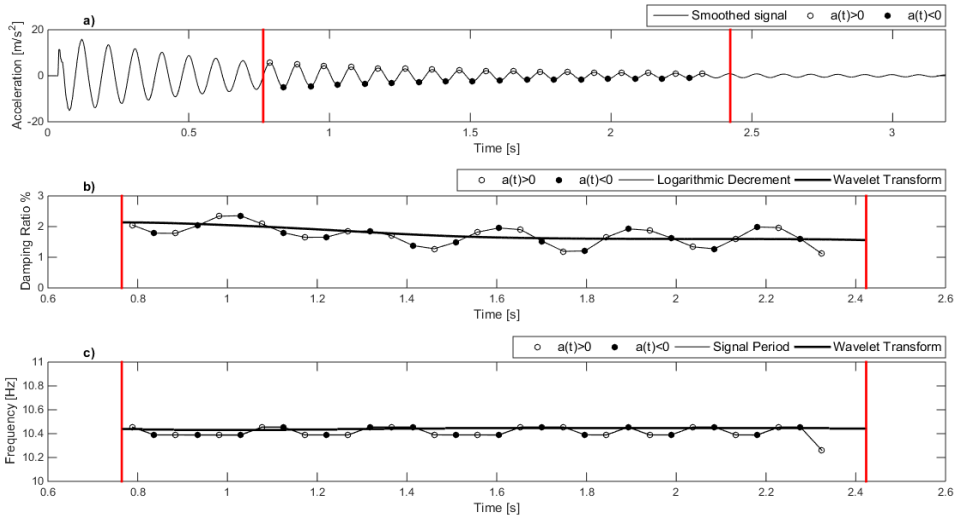

Figure 5 – a) TMD's acceleration, b) damping ratio and c) damped frequency under an impulsive shock for $D_1 = 0.24\ mm$ and $D_2 = 5.15\ mm$

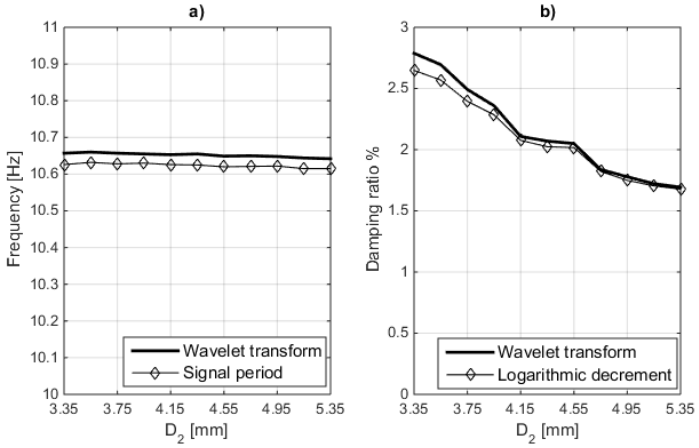

Figure 6 – TMD's damped frequency and b) TMD's damping ratio for fixed $D_1 = 0.24\ mm$ and varying D_2

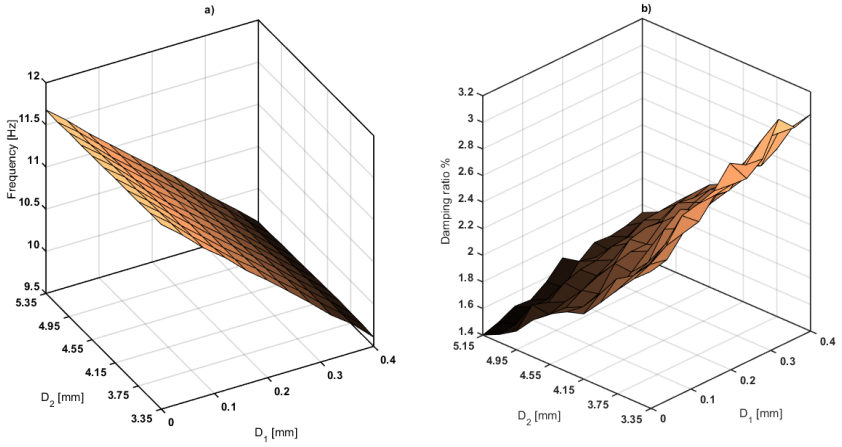

Figure 7 – a) TMD's damped frequency and b) damping ratio by varying cable stretching and magnet position

4. Conclusions

In this study, an experimental prototype of Tuned Mass Damper based on the damping effect of Eddy Currents is proposed. The eddy currents are induced by the movement of a conductor, which is the TMD's mass, within a stationary magnetic field. As a consequence, a magnetic field opposite to the flux change arises, together with a Lorentz force, which is opposite to the conductor movement. Several vibration tests were performed and the TMD's parameter estimation was carried out with the aid of the Wavelet transform. The research objective was to evaluate the influence of the cable level stress and of distance between the magnet and the conductive mass on the modal parameters. In this framework, not only the eddy currents were shown to be effective in order to furnish the damping to the TMD device, but also the damping achieved was shown to be viscous. In particular, the damping ratio obtained depends on the distance of the circular magnet from the damper mass and decreases non-linearly with the considered gap. Conversely, the TMD's stiffness given by the slender cable connected to the mass increases linearly when the cable tensile stress is augmented.

Bibliography

[1] A. Allani, F. Maceri, P. Argoul. Optimization of one or multiple tuned mass dampers, XVIIIth symposium Vibrations, Chocs et Bruit & ASTELAB, Vibrations, SHocks and NOise – VISHNO, 1-19, 2012.

[2] J. Bae, M. K. Kwak, D. J. Inman. Vibration suppression of a cantilever beam using eddy current damper, Journal of Sound and Vibration, Elsevier, 805-824, 2005.

[3] J. Bae, J. Hwang, J. Roh, J. Kim, M. Yi, J. H. Lim. Vibration suppression of a cantilever beam using magnetically tuned-mass-damper, Journal of Sound and Vibration, Elsevier, 5669-5684, 2012.

[4] J. Bae, J. Hwang, D. Kwag, J. Park, D. J. Inman. Vibration Suppression of a Large Beam Structure Using Tuned Mass Damper and Eddy Current Damping, Shock and Vibration, IOS Press, Article ID 893914 10 pages, 2014.

[5] B. Ebrahimi, M. B. Khamesee, F. Golnaraghi. Design and modeling of a magnetic shock absorber based on eddy current damping effect, Journal of Sound and Vibration, Elsevier, 875-889, 2008.

[6] K. E. Graves, D. Toncich, P. G. Iovenitti. Theoretical comparison of motional and transformer EMF device damping efficiency, Journal of Sound and Vibration, Elsevier, 441-453, 2000.

[7] G. L. Larose, A. Larsen, E. Svensson. Modelling of tuned mass dampers for wind-tunnels tests on a full-bridge aeroelastic model, Journal of Wind Engineering and Industrial Aerodynamics, Elsevier, 427-437, 1995.

[8] T. Le, P. Argoul. Continuous wavelet transform for modal identification using free decay response, Journal of Sound and Vibration, Elsevier, 73-100, 2004.

[9] H. A. Sodano, J. Bae, Eddy Current Damping in Structures, The Shock and Vibration Digest, EBSCO Publishing, 469-478, 2004.

[10] H. A. Sodano, J. Bae, D. J. Inman, W. Keith Belvin. Concept and model of eddy current damper for vibration suppression of a beam, Journal of Sound and Vibration, Elsevier, 1177-1196, 2005.

[11] Z. Wang, Z. Chen, J. Wang. Feasibility study of a large-scale tuned mass damper with eddy current damping mechanism, Earthquake Engineering and Engineering Vibration, Springer, 391-401, 2012.